

VOLCANIC EXPLOSION CLOUDS: DENSITY, TEMPERATURE, AND PARTICLE CONTENT ESTIMATES FROM CLOUD MOTION

Lionel Wilson

Lunar and Planetary Unit, Department of Environmental Sciences  
University of Lancaster, Lancaster, LA1 4YQ, England

Stephen Self

Department of Geology, Arizona State University, Tempe, Arizona 85281

**Abstract.** Photographic records of 10 vulcanian eruption clouds produced during the 1978 eruption of Fuego Volcano in Guatemala have been analyzed to determine cloud velocity and acceleration at successive stages of expansion. Cloud motion is controlled by air drag (dominant during early, high-speed motion) and buoyancy (dominant during late motion when the cloud is convecting slowly). Cloud densities in the range 0.6 to 1.2 times that of the surrounding atmosphere were obtained by fitting equations of motion for two common cloud shapes (spheres and vertical cylinders) to the observed motions. Analysis of the heat budget of a cloud permits an estimate of cloud temperature and particle weight fraction to be made from the density. Model results suggest that clouds generally reached temperatures within 10 K of that of the surrounding air within 10 seconds of formation and that dense particle weight fractions were less than 2% by this time. The maximum sizes of dense particles supported by motion in the convecting clouds range from 140 to 1700  $\mu\text{m}$ .

Introduction

During an airborne volcano plume sampling experiment in Guatemala [Rose et al., 1978, 1979], small vulcanian explosions from Fuego Volcano (at 3763-m altitude) were filmed at one frame per second. The film sequences were taken as part of a multidisciplinary study by scientists from NCAR, USGS, NASA, and several colleges and universities during February, 1978, using a specially equipped NCAR Queen Air aircraft (see abstracts of AGU Symposium 'Airborne Sampling of Eruption Clouds of Explosive Volcanoes' [Cadle and Rose, 1978]). Instrumentation aboard the Queen Air monitored air speed, temperature, altitude, and position. The camera used was a fixed-position Flight Research model 4 35-mm time-lapse camera, mounted just inside a port window of the aircraft. Cloud dimensions and heights were measured on the film frames relative to the Fuego summit crater, which is  $150 \pm 5$  m in diameter. Perspective corrections were applied as necessary.

The films record Fuego in a mild state of eruption following earlier, quite violent vulcanian eruptions in late January 1978 [SEAN, 1978]. Vulcanian explosions may be defined [Self et al., 1979] as discrete volcanic explosions commonly producing pyroclastic ejecta with a relatively large (up to 80%) nonjuvenile component. During active periods, intervals between explosions vary from less than 1 min to about 1 day. Such

activity is generally readily distinguishable from strombolian explosive activity in which the ejecta consist almost entirely of incandescent juvenile debris expelled in pulses at intervals of much less than 1 s to a few minutes.

Many small vulcanian explosions, each producing a discrete, uniformly grey and apparently homogeneous cloud of released gas and particles, were photographed from about 1-km distance on February 19, 24, and 27, 1978, and analyses of 17 of these were made. Cloud diameters ranged from 10 to 15 m just above the crater rim to 50 to 70 m at heights up to 150 m. Rise velocities generally decreased by a factor of 3-5 over this vertical distance from initial values in the range 5 to 30 m/s. The explosions can be modeled as instantaneous sources of particles and gas.

Theory of Cloud Motion

The motion of a discrete explosion cloud as it emerges from the vent can be studied if the following simple approximations are made: (1) the cloud decompresses to atmospheric pressure quickly (this can be seen to be the case in the present study, as there is little sudden lateral expansion of plumes at the vent); (2) the cloud is treated as a rigid, incompressible 'object' of defined shape. The latter approximation is valid if velocities are well below the speed of sound (true in all cases filmed) but becomes increasingly inadequate with time after emergence as spatial gradients develop in pyroclast number density, particle size, water vapor content, and temperature. It is stressed that the presently proposed model cannot be applied to eruption clouds generated by relatively steady release of gas and pyroclasts from vents.

Two cloud shapes commonly occurred: a sphere or a vertical cylinder. The equations of motion for the two cases are found by equating the product of mass and acceleration to the total forces acting on the cloud (atmospheric drag, gravity, and buoyancy). For a sphere,

$$\frac{4}{3} \pi r^3 \beta \frac{du}{dt} = -\frac{1}{2} \alpha \pi r^2 W^2 C_s - \frac{4}{3} \pi r^3 (\beta - \alpha)g \quad (1)$$

i.e.,

$$\frac{\beta}{\alpha} = \frac{g - 3 C_s W^2 / 8r}{g + du/dt} \quad (2)$$

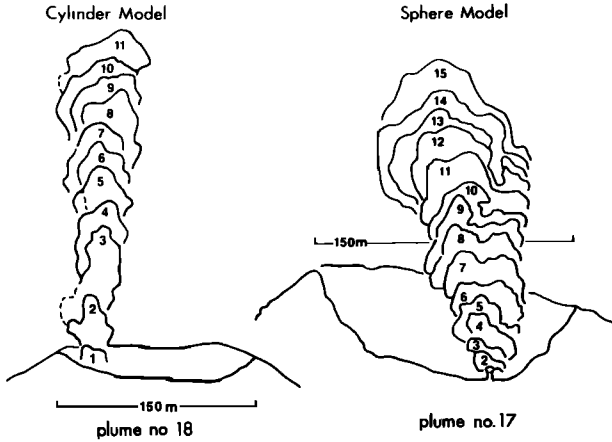


Fig. 1. Successive images for a sphere and cylinder cloud: 150-m scale shows crater of Fuego. Frame interval is 1 s.

the cloud is  $du/dt$  (negative if the cloud is decelerating), and the dimensionless drag coefficient  $C_d$  for a sphere is about 0.47.  $W$  is the relative velocity of the leading edge of the cloud and the air, and  $u$  the velocity of the cloud center. For a vertical cylinder the equivalent equation to (2) is

$$\frac{\beta}{\alpha} = \frac{g - C_d W^2/2L}{g + du/dt} \quad (3)$$

Here the drag coefficient  $C_d$  is about 1.0.

In the early part of the motion of a volcanic explosion cloud it is common for the second term on the right-hand side of (1) (representing buoyancy) to be negligible compared with the other two terms. The resulting period of rapid deceleration has been called the 'gas thrust' phase of the motion [Sparks and Wilson, 1976]. Later in the motion the term on the left-hand

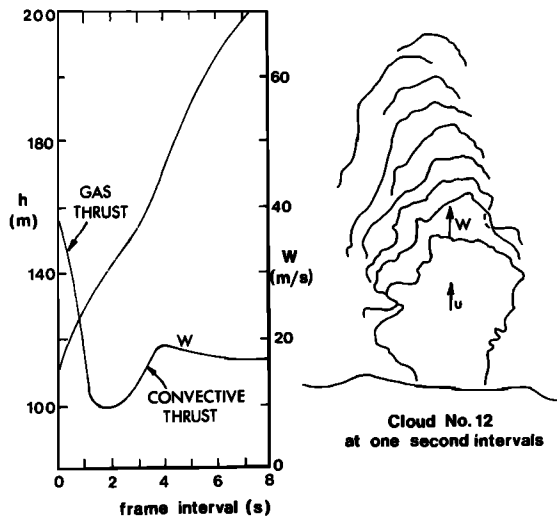


Fig. 2. Results of analysis of a cloud (sphere model) showing successive images (right) and the plot of height above crater ( $h$ ) and velocity of leading edge of cloud ( $W$ ) against time (left):  $u$  is velocity of cloud center.

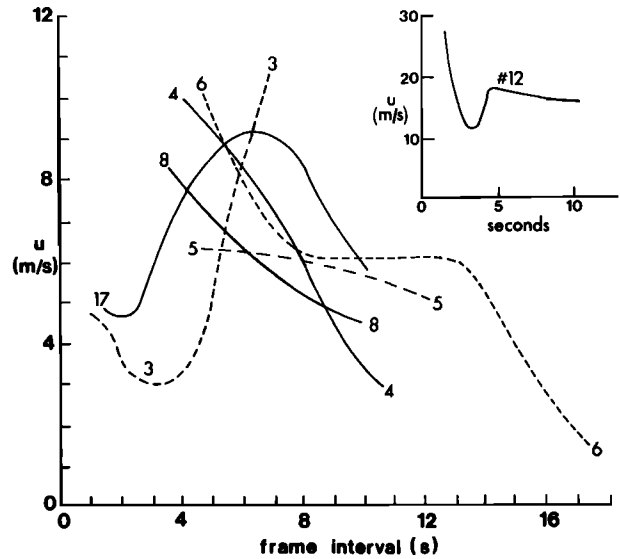


Fig. 3. Velocity of cloud center ( $u$ ) versus frame interval (time) in s for six of the slower clouds, showing a variety of behavior of speed of rise: Inset: one of the faster clouds analyzed. Initial velocities of 40–50 m/s are implied for plume 12. Solid curve indicates sphere model used; dashed curve, cylinder model. Numbers by curves identify clouds.

side (representing acceleration) becomes negligible, and the cloud convects upward at near-constant velocity in the 'convective thrust' phase.

For many clouds studied, all the parameters needed to solve (2) or (3) can be measured directly from the photographic film. The appropriate shape (sphere or cylinder) is fitted to each successive image (Figure 1) and the cloud center and top are measured above a reference point (the crater rim). Only clouds that maintain a simple shape can be analyzed in this way. Variations in height of cloud top and cloud center above crater rim as a function of time yield values for  $u$  and  $W$  (Figure 2). The slope of graphs of  $u$  against  $t$  (Figure 3) gives acceleration ( $du/dt$ ), hence the ratio of cloud density to air density ( $\beta/\alpha$ ) can be determined for each frame by substituting values of  $du/dt$  into the appropriate equation ((2) or (3)). Table 1 shows the variation of  $\beta/\alpha$  with time for four clouds. These analyses were performed on clouds rising above the crater rim. The actual vent for the eruptive mixture is known to be a few tens of meters below the rim; hence many clouds had already passed through the violent deceleration of the gas thrust phase before they were visible above the rim.

The relation of  $\beta/\alpha$  to other parameters can be investigated by considering the behavior of temperature within the eruption clouds. After a few seconds of rise, a cloud consists essentially of incorporated air plus those particles that have not fallen out of the cloud. As the air temperature rises from an ambient value  $\theta_a$  to a new value  $\theta$ , the air density will decrease from  $\alpha$  to  $(\alpha \theta_a/\theta)$ . If the gas weight fraction of the cloud is  $n$ , the particle weight fraction is  $(1-n)$  and the bulk density  $\beta$  is given by

TABLE 1. Selected Cloud Motion Analyses

Cloud No.	Model Shape	Frame No.	$\beta/\alpha$	Cloud Rise Velocity $u$ , m/s
3	Cylinder	1	0.728	4.5
		2	0.972	4.2
		3	0.983	3.0
		4	0.843	3.5
		5	0.727	5.0
		6	0.593	8.0
		7	0.560	10.0
4	Sphere	4	0.996	10.0
		5	0.932	9.3
		6	0.845	8.5
		7	0.922	7.3
		8	1.083	5.8
		9	1.091	4.4
6	Cylinder	5	0.732	10.0
		6	0.762	8.0
		7	0.924	7.0
		8	0.919	6.0
		9	0.908	6.0
		10	0.931	6.0
		11	0.942	6.0
		12	0.942	6.0
		13	0.985	6.0
		14	1.038	5.5
8	Sphere	4	0.750	8.0
		5	0.877	7.0
		6	0.946	6.5
		7	0.972	6.0
		8	0.996	5.0
		9	0.983	4.5
		10	0.985	4.5

are greater than 0.5 and mostly close to 1: at the height of the summit of Fuego,  $\alpha$  is about  $0.7 \times 10^{-3} \text{ g cm}^{-3}$ , but  $\rho$  is about  $2 \text{ g cm}^{-3}$ , so  $\alpha/\rho$  is  $<0.001$ ; hence  $(1-n) \alpha/\rho$  is always  $\ll \alpha/\beta$  and can be neglected, giving

$$\alpha/\beta = n\theta/\theta_a \tag{7}$$

Values for  $n$  must lie between 0 and 1 and presumably increase with time from a value in the range 0.01 to 0.05 (an approximate magmatic gas content [Anderson, 1975; Self et al., 1979]) to close to unity as the cloud becomes increasingly air dominated. Given a range of values for  $n$ , equations (6) and (7) can be used to estimate successive values of  $\theta/\theta_a$  and  $\beta/\alpha$ . Model values of  $\beta/\alpha$  can be compared to values estimated from the photographic records using equations (2) or (3). The only remaining unknown is the value to be adopted for  $\theta_s/\theta_a$  in (6). If  $\theta_s = 1100^\circ\text{C}$  (1373 K) and  $\theta_a = 0^\circ\text{C}$  (273 K), then  $\theta_s/\theta_a = 5.0$ ; if  $\theta_s$  is as low as  $850^\circ\text{C}$  (1123 K) and  $\theta_a$  as large as  $15^\circ\text{C}$  (288 K), then  $\theta_s/\theta_a = 3.9$ . These two values probably bracket the range of reasonable possibilities. Table 2 shows some values of  $\theta/\theta_a$  and  $\beta/\alpha$  for  $\theta_s/\theta_a = 4.0, 4.5, 5.0,$  and  $5.5$ ; the increase in  $n$  from 0.01 to 1.0 documents the increasing content of air in the plume. Model variations in cloud density and temperature are shown in Figure 4, using a value of  $\theta_s$  of  $1050^\circ\text{C}$  (1323 K), which is typical for Fuego magma [W. I. Rose, personal communication, 1979].

It will be noted that if  $\theta/\theta_a$  is eliminated between (6) and (7), the expression for  $n$  is quadratic. The requirement that the quadratic have real roots means that a restriction exists on  $\beta/\alpha$ : for any chosen value of  $\theta_s/\theta_a$ ,  $\beta/\alpha$  must always be greater than or equal to a minimum value given by

$$\frac{\beta}{\alpha} \geq (\theta_a)^2/\theta_s [\theta_s/\theta_a (1 + S_a/S_s) - 2 S_a/S_s + 2 \sqrt{S_a/S_s (\theta_s/\theta_a - 1) (\theta_s/\theta_a - S_a/S_s)}] \tag{8}$$

$$\frac{1}{\beta} = \frac{n}{\alpha \theta_s/\theta} + \frac{(1-n)}{\rho} \tag{4}$$

i.e.,

$$\frac{\alpha}{\beta} = n \theta/\theta_a + \frac{(1-n)\alpha}{\rho} \tag{5}$$

If the clasts removed from the cloud at any stage contribute negligible heat to the cloud, then  $\theta$  is obtained by equating the heat lost by clasts  $[(1-n) S_s (\theta_s - \theta)]$  to the heat gained by air  $[n S_a (\theta - \theta_a)]$ .

$$\frac{\theta}{\theta_a} = \frac{n S_a/S_s + (1-n) \theta_s/\theta_a}{1 + n (S_a/S_s - 1)} \tag{6}$$

where  $S_a$  and  $S_s$  are the specific heats at constant pressure of air and rock, the adopted values being 0.24 and 0.20 cal/g/K, respectively. A simplification can be made to (5) because all values of  $\beta/\alpha$  encountered in the cases analyzed

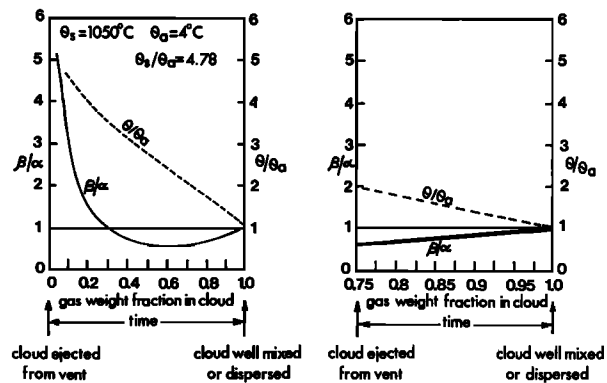


Fig. 4. Theoretical behavior of plume/air density ratio  $\beta/\alpha$  (solid line) and temperature ratio,  $\theta/\theta_a$  (dashed line). Values chosen for  $\theta_s$  and  $\theta_a$  are typical of Fuego conditions (see text). (Left) For  $n$  increasing to unity from an initial value less than 0.1. (Right) For  $n$  increasing from an initial value of 0.75. (Note: abscissa is in values of  $n$ , but this also represents increasing time (for the plumes analyzed this was usually 10–15 s).

TABLE 2. Theoretical Eruption Cloud Parameters

n	$\theta_s/\theta_a = 4$		$\theta_s/\theta_a = 4.5$		$\theta_s/\theta_a = 5$		$\theta_s/\theta_a = 5.5$	
	$\theta/\theta_a$	$\beta/\alpha$	$\theta/\theta_a$	$\beta/\alpha$	$\theta/\theta_a$	$\beta/\alpha$	$\theta/\theta_a$	$\beta/\alpha$
0.01	3.98	25.156	4.47	22.367	4.97	20.134	5.46	18.306
0.05	3.87	5.162	4.35	4.594	4.83	4.139	5.31	3.765
0.1	3.75	2.669	4.20	2.378	4.66	2.145	5.12	1.953
0.3	3.21	1.037	3.58	0.931	3.95	0.844	4.32	0.772
0.5	2.64	0.758	2.91	0.687	3.19	0.628	3.46	0.578
0.7	2.02	0.707	2.19	0.652	2.36	0.605	2.53	0.564
0.8	1.69	0.738	1.81	0.691	1.92	0.649	2.04	0.612
0.9	1.35	0.820	1.41	0.786	1.47	0.755	1.53	0.726
0.95	1.18	0.893	1.21	0.871	1.24	0.850	1.27	0.830
0.99	1.04	0.975	1.04	0.969	1.05	0.964	1.05	0.958
1.00	1.00	1.000	1.00	1.000	1.00	1.000	1.00	1.000

Values of the minimum for  $\beta/\alpha$  expected for  $\theta_s/\theta_a = 4.0, 4.5, 5.0,$  and  $5.5$  are 0.705, 0.647, 0.597, and 0.554, respectively.

#### Numerical Results

Data in Table 1 can be compared with the theoretically expected trends in Table 2 and Figures 4 and 5, where theoretical and experimental results are seen to be similar. Most clouds cannot be tracked for the first few frames, as they are obscured by other clouds and some clouds, e.g., 5, 6, and 8, have already reached their minimum density by the time they can be tracked, implying that they contain at least 70 wt % gas (i.e., mainly air), at a temperature of less than about  $2\theta_a$ . If we assume  $\theta_a = 4^\circ\text{C}$  (277 K), the average temperature at 3700 m measured in flight, then at this stage,  $\theta < 281^\circ\text{C}$  (554 K). In the following 5 to 10 seconds the gas weight fraction increases to at least 98% as  $\beta/\alpha$  approaches 1: values slightly greater than 1 are theoretically impossible at this stage, so the experimental values up to 1.15 indicate either that the model assumptions have become inadequate by this stage or that errors up to about 15% are present in the calculated values of  $\beta/\alpha$ . Temperatures at this stage fall to less than  $1.03\theta_a$ , i.e., to within 10 K of the ambient temperature. Condensation of the water vapor component of the magmatic gas must occur in this period, liberating further heat, but as the weight per unit volume of magmatic steam is much less than the weight of added air, the effect is small. Observations show that the eruption clouds disperse as  $\beta$  approaches or becomes greater than  $\alpha$ .

Other clouds, e.g., 3 and 4 (Figure 5), pass through minimum density in the part of the motion tracked and are accelerating into the convective thrust phase as incorporated air is heated. The minimum densities are  $\beta/\alpha = 0.56$  and  $0.845$ , respectively. The first of these values is within

the range expected from equation (8), 0.55 to 0.7, but the second is rather high, implying that either the initial explosion products were cooler than usual or the surrounding air into which the explosion cloud emerged was warmer than assumed. The latter possibility can easily result when two explosions follow one another closely in time; the former circumstance would be most easily explained if some meteoric water from the volcanic edifice were involved in the explosions [Nairn and Self, 1978; Self et al., 1979].

Rose et al. [1979] have proposed that gas-pyroclast mixtures discharged during the 1978 Fuego eruption were characterized by initial gas contents ranging up to 75 wt % ( $n = 0.75$ ). Such a high initial gas content would produce a plume with a low initial density. Comparison of

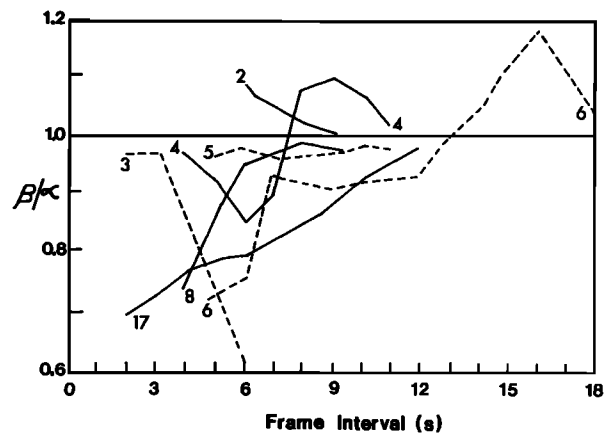


Fig. 5. Experimental results for plume/air density ratio  $\beta/\alpha$  with time. Numbers on curves refer to individual clouds analyzed. Solid curve indicates sphere model used; dashed curve, cylinder model.

TABLE 3a. Particle Sizes in Convecting Plumes: Plumes From February 27, 1978, Analyzed by Film

Plume Number	Plume Velocity, m/s	Diameter of Largest Particle Supported, $\mu\text{m}$
17	7.5	1725
5	5.2	890
8	4.5	670
4	2.8	360
6	1.0	140

Figures 4 and 5 suggests that some of the photographed plumes result from explosions of magma with high initial gas content (those with  $\beta/\alpha$  always  $<1.0$ ); others result from explosions with low initial gas content (those with  $\beta/\alpha$  initially  $>1.0$ ).

An estimate of the size of the largest particle supported in a convecting cloud can be made by equating the terminal velocity of the particle to the cloud rise velocity ( $u$ ). This method is not exact, as turbulent effects within the plume are ignored. For the clouds which are dispersing in the analyzed frames, e.g., 4, 5, 6, and 8, the cloud density is essentially atmospheric, i.e.,  $0.7 \times 10^{-3} \text{ g cm}^{-3}$ , in the last frame analyzed. Assuming a typical irregular shape [Wilson and Huang, 1979] and particle density of  $2 \text{ g cm}^{-3}$ , terminal velocities of particles can be found by the method of Walker et al. [1971]. The values, which range from 140 to 1700  $\mu\text{m}$  (Table 3), are comparable to particle sizes observed in cloud samples obtained during the aircraft missions by passing an air stream through Fluoropore filters [Self, 1978; Rose et al., 1979]. All samples taken were within plumes that had aged at least 10 s. In general, the size range of particles was  $<900 \mu\text{m}$ ; examples of maximum particle diameters are shown in Table 3. Only one of the analyzed clouds (plume 17) yielded particle sizes in excess of 1 mm, the remainder being in the sub-500  $\mu\text{m}$  range.

### Conclusions

Chouet et al. [1974] performed photoballistic studies of strombolian eruptions and discovered that the initial volume ratio of magmatic gas to solid particles within the erupted gas-pyroclast mixture could be large ( $>>1$ ). Their analysis was concentrated on the dynamic conditions within the volcanic jet. Blackburn et al. [1976] analyzed film of the motion of strombolian explosion clouds at relatively greater heights above the vent where air was being mixed into the clouds. This paper demonstrates that similar, quantitative estimates of parameters within convecting eruption clouds from vulcanian explosions can also be made from photographic records providing appropriate assumptions are made.

The suggestion of Rose et al. [1978], based on masses of gas to particles sampled in the plumes, that the initial gas content of the erupted mixture was as high as 75 wt %, implies that the 1978 Fuego explosions may be somewhat akin to

TABLE 3b. Particle Sizes in Convecting Plumes: Plumes Sampled on Filters From Aircraft

Date of Flight 1978	Diameter of Largest Particle Sampled, $\mu\text{m}$
February 20	275
February 23	260
February 28	950

strombolian activity, but modified by internal vent conditions, so that only convecting velocities are observed above the vent rim. There are other differences, however:

1. The small explosions described here have a higher proportion of nonjuvenile material in the ejecta than strombolian fire fountains [Blackburn et al., 1976; Chouet et al., 1974]. This suggests incorporation of vent wall material due to explosions deep in the conduit, whereas strombolian explosions essentially take place at the surface.

2. Fragmentation of magma in the Fuego explosions is more complete than in the strombolian case. Studies of the Heimaey strombolian eruption in 1973 [Self et al., 1974] showed that a very small proportion of the magma was fragmented to  $<1 \text{ mm}$  in size. Available studies of vulcanian-type deposits [e.g., Nairn and Self, 1978; Rose et al., 1978] indicate that  $>50\%$  by weight of the pyroclasts are  $<1 \text{ mm}$  in size, and this is borne out by particle size studies of the 1978 plume samples [S. Self and W. I. Rose, unpublished manuscript, 1979]. This may promote more vigorous convection within vulcanian eruption clouds due to the more efficient heat transfer between the particle and gas phases [Wilson et al., 1978].

3. The initiation of some explosions may involve meteoric water held in the superstructure of the volcano [Nairn and Self, 1978; Self et al., 1979]. Variation of initial gas contents within gas-pyroclast mixtures at Fuego, inferred from plume motion analysis of many individual explosions, could be explained by differing amounts of meteoric water incorporated into the mixture. More likely, varying proportions of magmatic gas to solid magma result from random mixing that occurs in the upper portions of the magma column.

Explosion clouds from the 1978 Fuego activity decelerate and mix very rapidly with air (Figures 3 and 5), the cloud temperature also reaches ambient within 10-15 s. The comparatively low velocities of the clouds, dominated by convective rise, allow only submillimeter particles to be supported to any height above the vent. The observations and the theory presented herein are also applicable to the early parts of the motion of much more violent and vigorously convecting explosion clouds from volcanoes.

### Notation

- $r$  radius of spherical cloud
- $u$  velocity of center of cloud
- $W$  velocity of leading edge of cloud

t	time
$\beta$	density of volcanic cloud or plume
$\alpha$	density of atmosphere
$C_s, C_c$	drag coefficient for sphere, cylinder model
L	length dimension of cylinder
$\theta$	temperature within volcanic cloud
$\theta_a$	temperature of atmosphere
n	weight fraction of gas (magmatic plus incorporated air) within volcanic cloud
$\rho$	average density of volcanic ejecta
S	specific heat of rock
$S_a$	specific heat of air

**Acknowledgments.** We would like to thank the pilot on this experiment, Lester Zinzer, for his cooperation and expertise in helping us obtain the film and Edward N. Brown for organizing the photographic equipment: both are from NCAR Research Aviation Facility. William Rose, Mark Settle, and an anonymous referee critically reviewed the manuscript, and Dorothy R. Wilson assisted with film analysis. Self acknowledges NASA grant NSG5145 for support during this study; Wilson received partial support from NSF grant EAR76-22319.

#### References

- Anderson, A. T., Some basaltic and andesitic gases, *Rev. Geophys. Space Phys.*, **8**, 37, 1975.
- Blackburn, E. A., L. Wilson, and R. S. J. Sparks, Mechanisms and dynamics of strombolian activity, *J. Geol. Soc. London*, **132**, 429-440, 1976.
- Briggs, G. A., Plume rise, Critical Review Series, Rep. TID-25075, pp. 1-81, At. Energy Comm., Washington, D. C., 1969.
- Cadle, R. D., and W. I. Rose, Jr., Airborne sampling of eruption clouds of explosive volcanoes, *EOS Trans. AGU*, **59**, 1221-1223, 1978.
- Chouet, B., N. Hamisevicz, and T. R. McGetchin, Photoballistics of volcanic jet activity at Stromboli, Italy, *J. Geophys. Res.*, **79**, 4961-4976, 1974.
- Nairn, I. A., and S. Self, Explosive eruptions and pyroclastic avalanches from Ngauruhoe in February 1975, *J. Volcanol. Geotherm. Res.*, **3**, 39-60, 1978.
- Rose, W. I., Jr., Santiaguito volcanic dome complex, Guatemala, *Geol. Soc. Amer. Bull.*, **83**, 1413, 1972.
- Rose, W. I., R. D. Cadle, A. L. Lazrus, L. E. Heidt, B. J. Huebert, R. E. Stoiber, S. Self, G. Bratton, R. L. Chuan, D. C. Woods, I. Friedman, and L. Wilson, 1978 Volcanic eruption cloud sampling project, *Geol. Soc. Amer. Abstr. Programs*, **10**(7), 480, 1978.
- Rose, W. I., Jr., R. D. Cadle, D. C. Woods, and R. L. Chuan, Small particles in volcanic eruption clouds, *Amer. J. Sci.*, **280**, in press, 1980.
- SEAN, Scientific Event Alert Network, vol. 3, nos. 1 and 2, Smithsonian Institution, Washington, D. C., 1978.
- Self, S., Particle size distribution and morphology of ash in the Fuego and Santiaguito plumes (abstract), *EOS Trans. AGU*, **59**, 1222, 1978.
- Self, S., R. S. J. Sparks, G. P. L. Walker, and B. Booth, The 1973 Heimaey strombolian scoria deposit, Iceland, *Geol. Mag.*, **111**, 539, 1974.
- Self, S., L. Wilson, and I. A. Nairn, Vulcanian eruption mechanisms, *Nature*, **277**, 440, 1979.
- Sparks, R. S. J., and L. Wilson, A model for the formation of ignimbrite by gravitational column collapse, *J. Geol. Soc. London*, **132**, 441, 1976.
- Walker, G. P. L., L. Wilson, and E. L. G. Howell, Explosive volcanic eruptions, I, The rate of fall of pyroclasts, *Geophys. J. Roy. Astron. Soc.*, **22**, 377, 1971.
- Wilson, L., and T. C. Huang, The influence of shape on the settling velocity of volcanic ash particles, *Earth Planet. Sci. Lett.*, **44**, 311-324, 1979.
- Wilson, L., R. S. J. Sparks, T. C. Huang, and N. D. Watkins, The control of volcanic column heights by eruption energetics and dynamics, *J. Geophys. Res.*, **83**, 1829-1836, 1978.

(Received January 31, 1980;  
accepted February 5, 1980.)